performed a PCR at RCA-specific conditions using the bacterial primer gm3f (ref. 26) and rca994r. Sequencing primers were gm3f, rca418f and rca994r. The affiliation of the sequences with the RCA cluster was checked by phylogenetic analysis.

Quantification of RCA phylotypes

We developed a specific PCR approach to estimate the abundance of the RCA phylotypes relative to total bacterial 16S rRNA genes based on serial dilution of extracted DNA. Alternate 1:5 and 1:2 dilution steps to extinction were applied in triplicates, to 10^7-fold dilution or higher. PCRs with bacterial and RCA-specific primers were performed simultaneously using 60 °C for annealing. We used a PCR with primer pair 341f–907r for comparison because it amplifies a fragment consisting of approximately 560 bp (RCA-PCR 570 bp), melting temperatures, T_m, are similar (rca418f $T_m = 56$ °C; rca994r $T_m = 54$ °C; 341f $T_m = 58$ °C; 907r $T_m = 54$ °C) and the two fragments overlap in the majority of their sequences. PCR products were analysed on the same agarose gels. Gel images were edited with GelComparII (Applied Maths). Only bands differing distinctly from background noise were treated as positive results. The fraction of RCA-specific relative to total bacterial 16S rRNA genes was determined as follows. Percentage of RCA 16S rRNA genes $= \mathrm{dil}_{\mathrm{Bacteria}}/\mathrm{dil}_{\mathrm{RCA}} \times 100$, where $\mathrm{dil}_{\mathrm{RCA}}$ is the highest dilution step in which RCA-specific 16S rRNA gene fragments were detected and $\mathrm{dil}_{\mathrm{Bacteria}}$ is the highest dilution step in which bacterial 16S rRNA gene fragments were detected. In all experiments, bacterial and RCA-cluster-specific genes were detected in all triplicates of the highest dilution steps in which they occurred.

RCA-specific oligonucleotides for FISH

Specific oligonucleotides were designed and specificity was checked as described for primer design. Owing to the low signal intensity of oligonucleotides used for the specific PCR approach, probe RCA826 was designed as 5′-ATACTTGCTGACGTCTGG-3′. In addition, probe ALF968, which targeted α-*Proteobacteria* labelled with Cy3, was applied[27]. FISH with the RCA-specific oligonucleotide labelled with Cy3 and unlabelled helper probes RCA808-H (5′-CATTCATCGTTTACGGTG-3′) and RCA845-H (5′-GGTGTGACACCAACAAGT-3′) was done as described[18]. Hybridization was done on quarters of 0.2 μm Nuclepore membranes at 46 °C for 5 h in hybridization buffer and 35% formamide. For negative controls, we used a Cy3-labelled non-EUB338 probe. The final concentration of each probe was 5 ng μl^{-1}. Washing and staining by DAPI was done essentially as described[28].

Phylogenetic analysis and tree construction

Obtained sequences were compared with sequences from public databases. Phylogenetic trees were constructed with the ARB software package. Sequences of >1,300 bp of at least two representative, validated type strains of every order and of representative phylotypes of the SAR116 and SAR11 clades of α-*Proteobacteria* were used, except clones SAR116 (479 bp) and SAR11 (1,107 bp). A sequence collection of γ-*Proteobacteria* served as outgroup. Alignment positions at which <50% of α-*Proteobacteria* sequences had the same residues were excluded to prevent uncertain alignments within highly variable positions.

Received 10 July; accepted 4 December 2003; doi:10.1038/nature02272.

1. Hagström, A. *et al.* Use of 16S ribosomal DNA for delineation of marine bacterioplankton species. *Appl. Environ. Microbiol.* **68,** 3628–3633 (2002).
2. Cottrell, M. T. & Kirchman, D. L. Community composition of marine bacterioplankton determined by 16S rRNA gene clone libraries and fluorescence *in situ* hybridization. *Appl. Environ. Microbiol.* **66,** 5116–5122 (2000).
3. Giovannoni, S. & Rappé, M. in *Microbial Ecology of the Oceans* (ed. Kirchman, D. L.) 47–84 (Wiley-Liss, New York, 2000).
4. Giovannoni, S. J., Britschgi, T. B., Moyer, C. L. & Field, K. G. Genetic diversity in Sargasso Sea bacterioplankton. *Nature* **345,** 60–63 (1990).
5. Morris, R. M. *et al.* SAR11 clade dominates ocean surface bacterioplankton communities. *Nature* **420,** 806–810 (2002).
6. Schut, F. *et al.* Isolation of typical marine bacteria by dilution culture: growth, maintenance, and characteristics of isolates under laboratory conditions. *Appl. Environ. Microbiol.* **59,** 2150–2160 (1993).
7. Muyzer, G. *et al.* in *Molecular Microbial Ecology Manual* (eds Akkermans, A. D. L., van, Elsas, J. D. & de Bruijn, F. J.) Ch. 3.4.4, 1–27 (Kluwer Academic, Dordrecht, 1998).
8. American Public Health Association. *Standard Methods for Examination of Water and Wastewater Including Bottom Sediments and Sludge* 604–609 (APHA, Washington DC, 1969).
9. Zubkov, M. V. *et al.* Linking the composition of bacterioplankton to rapid turnover of dissolved dimethylsulphoniopropionate in an algal bloom in the North Sea. *Environ. Microbiol.* **3,** 304–311 (2001).
10. González, J. M. *et al.* Bacterial community structure associated with a dimethylsulfoniopropionate-producing North Atlantic algal bloom. *Appl. Environ. Microbiol.* **66,** 4237–4246 (2000).
11. Bano, N. & Hollibaugh, J. T. Phylogenetic composition of bacterioplankton assemblages from the Arctic Ocean. *Appl. Environ. Microbiol.* **68,** 505–518 (2002).
12. Gosink, J. J., Herwig, R. P. & Staley, J. T. *Octadecabacter arcticus* gen. nov., sp. nov., and *O. antarcticus*, sp. nov. nonpigmented, psychrophilic gas vacuolate bacteria from polar sea ice and water. *Syst. Appl. Microbiol.* **20,** 356–365 (1997).
13. Fuchs, B. M., Zubkov, M. V., Sahm, K., Burkill, P. H. & Amann, R. Changes in community composition during dilution cultures of marine bacterioplankton as assessed by flow cytometric and molecular biological techniques. *Environ. Microbiol.* **2,** 191–201 (2000).
14. Gonzalez, J. M. & Moran, M. A. Numerical dominance of a group of marine bacteria in the α-subclass of the class *Proteobacteria* in coastal seawater. *Appl. Environ. Microbiol.* **63,** 4237–4242 (1997).
15. Rappé, M. S., Kemp, P. F. & Giovannoni, S. J. Phylogenetic diversity of marine coastal picoplankton 16S rRNA genes cloned from the continental shelf off Cape Hatteras, North Carolina. *Limnol. Oceanogr.* **42,** 811–826 (1997).
16. Longhurst, A. *Ecological Geography of the Sea* Ch. 10, 339–365 (Academic, San Diego, CA, 1998).
17. Staley, J. T. & Gosink, J. J. Poles apart: biodiversity and biogeography of sea ice bacteria. *Annu. Rev. Microbiol.* **53,** 198–215 (1999).
18. Fuchs, B. M., Glöckner, F. O., Wulf, J. & Amann, R. Unlabeled helper oligonucleotides increase the *in situ* accessibility to 16S rRNA of fluorescently labeled oligonucleotide probes. *Appl. Environ. Microbiol.* **66,** 3603–3607 (2000).
19. Beja, O. *et al.* Unsuspected diversity among marine aerobic anoxygenic phototrophs. *Nature* **415,** 630–633 (2002).
20. Kolber, Z. S. *et al.* Contribution of aerobic photoheterotrophic bacteria to the carbon cycle in the ocean. *Science* **292,** 2492–2495 (2001).
21. Ward, B. B. & O'Mullan, G. D. Worldwide distribution of *Nitrosococcus oceani*, a marine ammonia-oxidizing γ-proteobacterium, detected by PCR and sequencing of 16S rRNA and amoA genes. *Appl. Environ. Microbiol.* **68,** 4153–4157 (2002).
22. Kirchman, D. L. The ecology of *Cytophaga-Flavobacteria* in aquatic environments. *FEMS Microbiol. Ecol.* **1317,** 91–100 (2002).
23. Field, K. *et al.* Diversity and depth-specific distribution of SAR11 cluster rRNA genes from marine planktonic bacteria. *Appl. Environ. Microbiol.* **63,** 63–70 (1997).
24. Garcia-Martinez, J. & Rodriguez-Valera, F. Microdiversity of uncultured marine prokaryotes: the SAR11 cluster and the marine *Archaea* of Group I. *Mol. Ecol.* **9,** 935–948 (2000).
25. Selje, N. & Simon, M. Composition and spatio-temporal dynamics of particle-associated and free-living bacterial communities in the Weser estuary, Germany. *Aquat. Microb. Ecol.* **30,** 221–236 (2003).
26. Muyzer, G., Teske, A., Wirsen, C. O. & Jannasch, H. W. Phylogenetic relationships of *Thiomicrospira* species and their identification in deep-sea hydrothermal vent samples by denaturing gradient gel electrophoresis of 16S rRNA fragments. *Arch. Microbiol.* **164,** 165–172 (1995).
27. Glöckner, F. O., Fuchs, B. M. & Amann, R. Bacterioplankton compositions of lakes and oceans: a first comparison based on fluorescence *in situ* hybridization. *Appl. Environ. Microbiol.* **65,** 3721–3726 (1999).
28. Glöckner, F. O. *et al.* An *in situ* hybridization protocol for detection and identification of planktonic bacteria. *Syst. Appl. Microbiol.* **19,** 403–406 (1996).

Acknowledgements We thank R. Brinkmeyer, A. Bruns, B. Engelen, S. Germer, H.-P. Grossart, K. Pohlmann, U. Saint-Paul, G. Steward, M. Taylor, A. Teske and W. Zwisler for providing us with samples from various oceanic regions, A. Schlingloff for assistance in sequencing, and D. Dotschkal for FISH and *puf* gene analyses. We are grateful to D. L. Kirchman, M. A. Moran and U. Riebesell for suggestions on earlier versions of this manuscript. This work was supported by grants from the Deutsche Forschungsgemeinschaft.

Competing interests statement The authors declare that they have no competing financial interests.

Correspondence and requests for materials should be addressed to M.S. (m.simon@icbm.de). The sequences reported in this study are deposited under GenBank accession numbers AY165487–AY165505, AY145589 (DC5-80-3) and AY145625 (DC11-80-2).

Species-specific calls evoke asymmetric activity in the monkey's temporal poles

Amy Poremba[1], Megan Malloy[2], Richard C. Saunders[2], Richard E. Carson[3], Peter Herscovitch[3] & Mortimer Mishkin[2]

[1]*Behavioral and Cognitive Neuroscience, Department of Psychology, University of Iowa, Iowa City, Iowa 52242, USA*
[2]*Laboratory of Neuropsychology, National Institute of Mental Health, and* [3]*PET Department, Clinical Center, National Institutes of Health, Bethesda, Maryland 20892, USA*

It has often been proposed that the vocal calls of monkeys are precursors of human speech, in part because they provide critical information to other members of the species who rely on them for survival and social interactions[1,2]. Both behavioural and lesion studies suggest that monkeys, like humans, use the auditory system of the left hemisphere preferentially to process vocalizations[3,4]. To investigate the pattern of neural activity that might underlie this particular form of functional asymmetry in monkeys, we measured local cerebral metabolic activity while the animals listened passively to species-specific calls compared with a variety of other classes of sound. Within the superior temporal gyrus, significantly greater metabolic activity occurred

on the left side than on the right, only in the region of the temporal pole and only in response to monkey calls. This functional asymmetry was absent when these regions were separated by forebrain commissurotomy, suggesting that the perception of vocalizations elicits concurrent interhemispheric interactions that focus the auditory processing within a specialized area of one hemisphere.

Understanding where and how monkeys process auditory communicative signals could help delineate the precursor neural framework for the evolution of language. Because lateralization of language processing is a major cerebral organizing theme in humans, any similar asymmetry in monkeys could reflect an antecedent neural mechanism. Behavioural methods have indicated that macaques tend to turn the right ear to the source of species-specific vocalizations but not to the source of many other types of sound, suggesting that their left hemisphere is specialized for analysing vocalizations in particular[5,6]. This suggestion is consistent with lesion findings demonstrating that ablation of auditory cortex on the left but not on the right impairs the animal's ability to discriminate monkey calls[4].

We explored the physiology mediating this putative hemispheric specialization by injecting rhesus monkeys with radiolabelled 2-fluoro-2-deoxyglucose (FDG) immediately before exposing them to monkey vocalizations or other classes of sound, and then placing them in a positron emission tomography (PET) scanner to measure local cerebral metabolic activity[7]. On the basis of the results of an earlier metabolic (2-deoxyglucose) study of auditory processing in the monkey[8], we selected five regions along the length of the superior temporal gyrus (STG) and examined each of them for evidence of asymmetrical activation (see Methods).

Significantly greater activation on the left than on the right was evoked only by species-specific monkey vocalizations and, within the STG, only at the level of the dorsal temporal pole (Fig. 1 and Supplementary Table 1). This effect was not elicited by any of the other sound classes, which included simple and complex non-vocal sounds, phase-scrambled species-specific monkey vocalizations, human speech and ambient background noise (see Methods). The effect was not only specific to monkey calls, it was sufficiently strong to remain evident even when such calls were randomly intermixed with sounds from the other classes (Fig. 1 and Supplementary Table 1).

Comparison among the activity levels evoked by the different sound classes suggested that the asymmetry observed during vocalizations could be due to trans-commissural suppression of activity in the right temporal pole. That the forebrain commissures can mediate suppression of activity in one hemisphere by activity in the other was demonstrated by, among others, behavioural studies in the motor system using both transcranial magnetic stimulation and EEG[9,10]. To examine whether an interhemispheric suppression mechanism might have been operating in our study, we prepared monkeys with forebrain commissurotomy and then tested them in the same way we had tested the intact monkeys. No asymmetry was evident in the temporal poles of the commissurotomized cases; moreover, the activity of the right temporal pole was significantly higher in the commissurotomized than in the intact animals ($F_{1,9} = 9.295$, $P < 0.05$; Fig. 1). These findings thus provide some preliminary support for the notion that the processing of species-specific calls normally leads to trans-commissural suppression of activity in the right temporal pole.

The asymmetry in the intact animals was evident even when monkey calls were randomly intermixed with sounds from stimulus classes that did not evoke asymmetry, which implies that the relatively greater activity in the left temporal pole elicited by those calls results from a dynamic, stimulus-dependent, rather than a static, set-dependent, form of interhemispheric interaction. Stated another way, the interhemispheric interaction appears to be event-related rather than block-related, in the sense in which these terms are used in functional MRI studies[11], with the signal emerging from the summed activations evoked by the separated events of the same class, again as in functional MRI.

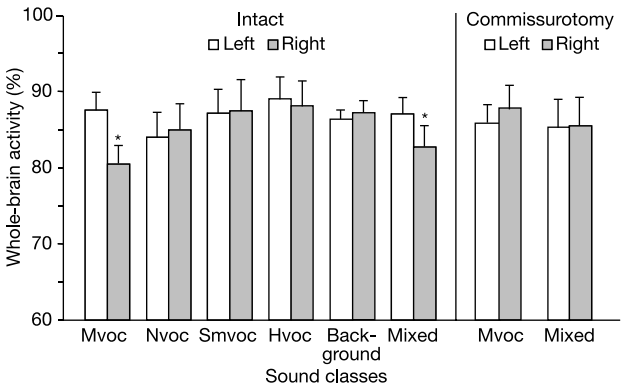

Figure 1 Metabolic activity (means and standard errors) in the monkey's dorsal temporal poles (sector 5 in the schematic brain view shown in Fig. 2) during presentation of six different classes of sound. In intact monkeys ($n = 8$), the left dorsal temporal pole was activated significantly more than the right only by species-specific monkey vocalizations, either when these were presented alone as in sound class Mvoc, or intermixed with a variety of other stimuli as in Mixed. In monkeys with forebrain commissurotomy ($n = 3$), neither of these two sound classes elicited significant asymmetric activity in the dorsal temporal pole. Activity levels were the same in both groups for the other sound classes: see Methods for descriptions of these. Asterisks indicate left activity significantly greater than right, corrected for multiple planned comparisons using Keppel's modification of the Bonferroni procedure[24].

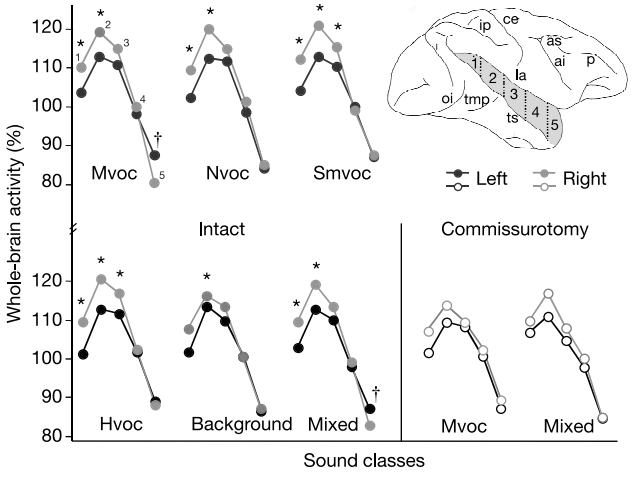

Figure 2 Metabolic activity in the left and right STG during presentation of six different sound classes (see Methods). The two rows of line graphs on the left depict activity in the intact monkeys to each of the six sound classes across STG sectors 1–5, which are demarcated on a lateral view of the monkey's brain at upper right (frontal lobe facing right). The two line graphs at the lower right depict activity in the commissurotomized monkeys to sound classes Mvoc and Mixed. The right STG is generally more active than the left across sectors 1–3 in both groups. Asterisks indicate right activity significantly greater than left, and daggers, left significantly greater than right, after correction for multiple planned comparisons using Keppel's modification of the Bonferroni procedure[24]. Sulcal abbreviations: ai, inferior limb of arcuate; as, superior limb of arcuate; ce, central; ip, intraparietal; la, lateral; oi, inferior occipital; p, principal; tmp, posterior middle temporal; ts, superior temporal.

It is noteworthy that greater activity in the left temporal pole than in the right was observed against the background of an opposite asymmetry elsewhere in the STG. The activity levels across the STG in both hemispheres took the shape of an inverted U (Fig. 2), with the activity on both sides rising from sector 1 (the most caudal level) to reach a peak in sector 2 (the level of the primary auditory projection areas), and then decreasing progressively across sectors 3–5 (the latter at the level of the temporal pole). This inverted-U pattern in the STG is a direct reflection of cortical metabolic activity[8]. Within the inverted U, the typical pattern of asymmetry —evoked across sectors 1–3 by all sound classes, including monkey calls—was greater activity on the right than on the left (Fig. 2). This right–left difference reached significance in sectors 1 and 2 for nearly every sound class. Interestingly, the monkeys with forebrain commissurotomy showed the same pattern (Fig. 2 and Supplementary Fig. 5), although here few of the differences reached significance. Presumably this is due at least in part to the small *N*, inasmuch as the magnitude and direction of the right–left differences in the three monkeys examined were highly similar to those in the eight intact monkeys (Fig. 3, Supplementary Figs 4 and 5 and Supplementary Tables 3 and 4).

Our results suggest that within the monkey's cortical auditory system, two different types of hemispheric lateralization coexist. One type, represented in the posterior portion of STG, apparently reflects right-hemisphere specialization for processing a wide variety of acoustic stimulus classes, including at least all those presented here. This putative specialization seems to be intrinsic to the right hemisphere, in that it is largely independent of concurrent interhemispheric interaction via the forebrain commissures; whether it is also independent of these commissures ontogenetically is at present unknown. The second type of lateralization, represented in the dorsal temporal pole—a late station in the putative ventral auditory pathway[8]—apparently reflects left-hemisphere specialization for processing monkey calls specifically. This second type of lateralization depends fully on the forebrain commissures, suggesting that, in the monkey, listening to a brief call can dynamically direct cortical processing to a unilateral substrate specialized for analysing that call. Whether the left dorsal temporal pole of the monkey is in fact necessary for analysing conspecific calls is yet to be determined.

Left-hemisphere specialization for processing of species-specific vocalizations may have an evolutionary origin in nonprimate mammals[12], paralleling that in birds[13]. Uncovering a neural basis for such specialization in monkeys, however, with their extensive auditory system[8] and their large number of distinct vocal communicative signals[14,15], could yield a special benefit. A number of studies have examined the responses to vocalizations of neurons located in the monkey's primary or secondary auditory processing areas[16–19]. Our results open up the possibility of characterizing such neuronal responses in a cortical region of the monkey that is not only a higher-order auditory processing area[8], but also one that could be a precursor for an acoustic language area in humans. □

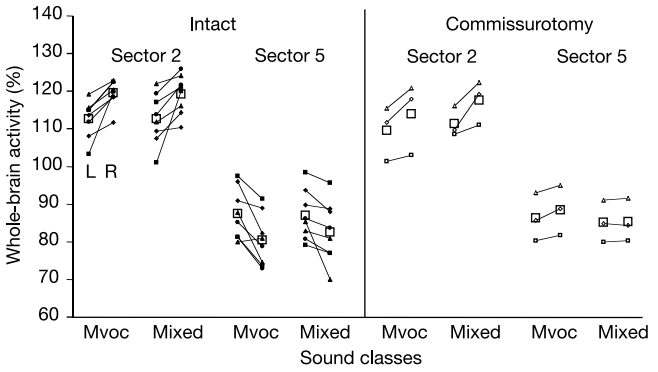

Figure 3 Metabolic activity values in sectors 2 and 5 for each individual subject for each of two sound classes, Mvoc and Mixed. Individual subject means for the left and right hemispheres are marked by the paired left and right (L and R) symbols, respectively, connected by solid lines. Group means for the left and right hemispheres are represented by the unconnected outline squares on the left and right, respectively. Sectors are demarcated on the lateral view of the monkey's brain in Fig. 2. Graphs indicate a consistent pattern of right activity greater than left across individual subjects in sector 2 (encompassing the primary auditory projection areas) for both sound classes and both groups. An equally consistent reversal of lateralization across individual subjects, with left hemisphere activity greater than right, is evident in sector 5 (temporal pole) for the same two sound classes, but for the intact monkeys only. The commissurotomy cases show no lateralization in sector 5.

Methods

Subjects and stimuli

The subjects were eight unoperated rhesus monkeys (*Macaca mulatta*, 5 female, 3 male) and three operated rhesus monkeys (2 female, 1 male) with complete forebrain commissurotomy, that is, combined transection of the corpus callosum and both the anterior and hippocampal commissures; the latter were tested 3–6 months after surgery. All procedures and animal care were conducted in accordance with the National Institutes of Health (NIH) Guide for the Care and Use of Laboratory Animals. All experimental procedures were approved by the NIMH Animal Care and Use Committee.

The monkeys were placed in a sound attenuation chamber (ambient background noise ~60 dB) and presented with six classes of auditory stimuli each in a separate scanning session: (1) 'Mvoc', species-specific, unfamiliar monkey vocalizations, consisting of coos (9%), grunts (10%), barks (26%), screams (37%), gurneys/warbles (13%) and harmonic arches (5%). (2) 'Nvoc', nonvocalizations, including such environmental stimuli as glass breaking, bells ringing, water dripping, electronic sounds and so on, as well as tones, frequency sweeps, and white noise. (3) 'Smvoc', scrambled monkey vocalizations (Supplementary Fig. 6) using the same stimuli as in the first class above, but phase-scrambled in the Fourier domain, while maintaining frequency information and stimulus amplitude envelopes equal to those in the original calls. (4) 'Hvoc', human vocalizations, consisting of both male and female voices uttering words, phrases and sentences. (5) 'Background', ambient background noise consisting mainly of white noise from the building's air-handling system. (6) 'Mixed', a randomized mixture of stimuli from the above classes (excluding the phase-scrambled calls) plus music and nonprimate animal vocalizations (birds, dogs, whales and so on).

About 20% of the stimuli in the mixed condition were from the class of monkey vocalizations. The stimuli, most of which lasted from about 1 to 3 s, were presented from two speakers 26.5 cm apart positioned on the front panel of the test chamber located 24 cm in front of the monkey. During the 25 min of passive listening on each scanning day, the stimuli were presented at a rate of approximately 12 per minute with a 3-s interstimulus interval, yielding approximately 300 stimuli lasting a total of about 12 min. The order of stimulus presentations within each sound class was the same for all animals. Scanning sessions for a given animal were separated by 60 days on average.

PET scan procedure and data analysis

On the day of the scan, the monkey was seated in a primate chair and placed in a sound-attenuated chamber. An intravenous cannula (Heplock) was inserted into the animal's leg, and 15 min later it was injected with 15 mCi of FDG, which is taken up both by neurons[20] and by glial cells involved in neurotransmitter metabolism[21], thereby providing a signal of energy consumption that increases linearly with functional activation. The acoustic stimuli were then presented, and after 25 min of passive listening, the monkey was sedated with ketamine (10 mg per kg intravenously) and a combined ketamine (8 mg per kg)/xylazine (0.4 mg per kg intramuscularly) solution and then transported to the PET scanner (GE Advance) for data acquisition. The animal's head was positioned within a stereotaxic head holder so as to obtain coronal images of FDG uptake.

Images were acquired in two-dimensional mode at two interleaved axial levels (2 mm apart) to provide maximal sampling. An 8-min transmission scan for attenuation correction at axial level 1 was followed by eight 5-min emission scans at alternating axial levels, followed by an 8-min transmission scan at level 2. This interleaved scan mode ensured that the average acquisition times postinjection at the two levels were nearly identical. The four image frames at each level were summed, and the slices from the two levels were interleaved to produce a final image volume of 70 slices with voxel dimension of 1 × 1 × 2 mm. The data were analysed using MedX 4.1 software. PET images were co-registered with each monkey's MRI scan using automated image registration[22]. MRI was performed in a 1.5-T Signa unit (GE Medical Systems), using a 5-inch surface coil. T1-weighted magnetic resonance images were obtained using three-dimensional volume SPGR pulse sequence (TE 6, TR 25, flip angle 30), field of view 11 cm, and slice thickness 1 mm. After co-registration, a normalized activity image was created by dividing the radioactivity of each voxel by the average concentration of whole-brain radioactivity. Owing to the linearity of the FDG model, these normalized values are nearly equal to normalized metabolic rates. (Normalized radioactivity values were used as the outcome

measure rather than absolute values of glucose utilization rates in order to avoid the effects of blood sampling during the scanning session.)

The regions of interest (ROIs), drawn on the coronal MRI scans for each monkey, were five sectors (1–5) along the lengths of the left and right STG. According to the architectonic schema of ref. 23, sector 1, the posterior auditory cortex, includes mainly the temporoparietal cortex, caudal parakoniocortex and retroinsular temporal area; sector 2, containing the primary auditory cortex, includes mainly lateral parakoniocortex, auditory koniocortex, lateral portion of temporalis superior (Ts) 3 and prokoniocortex; sector 3 includes the major portion of Ts3 and rostral parakoniocortex; sector 4 includes the major portion of (Ts2) and anterior portions of Ts3; and sector 5, the temporal pole, includes the major portion of (Ts1) and a small dorsal portion of proisocortex. These template ROIs were applied to each realigned and normalized PET scan.

The five sectors were preselected on the basis of their differential levels of 2-deoxyglucose uptake observed during an acute metabolic mapping study of auditory processing in monkeys[8]. In line with one of the premises of ROI analyses, each sector was treated as being independent of the others. Percentages of whole-brain activity for each sector were averaged across multiple coronal sections on which that ROI appeared, and comparisons were made between hemispheres with two-tailed paired *t*-tests. Keppel's modification of the Bonferroni procedure was used to correct the 'family-wise' error rate for multiple planned comparisons[24], as follows. The six different stimulus classes were entered as the experimental treatment, the number of degrees of freedom for this treatment source of variance ($6 - 1 = 5$) was multiplied by the standard critical probability level (0.05), and the product was divided by the number of planned comparisons (6), yielding a new, corrected, critical probability level of 0.042. In the case of the between-group comparison within sector 5, a three-way repeated-measures analysis of variance (ANOVA) was used with group (intact and commissurotomized), stimulus class (Mvoc and Mixed) and hemispheric side as the factors.

Received 24 July; accepted 5 December 2003; doi:10.1038/nature02268.

1. Cheney, D. L. & Seyfarth, R. M. *How Monkeys See The World* (Univ. Chicago Press, Chicago, IL, 1990).
2. Prell, C. G., Hauser, M. D. & Moody, D. B. Discrete or graded variation within rhesus monkey screams? Psychophysical experiment on classification. *Anim. Behav.* **63,** 47–62 (2002).
3. Ghazanfar, A. A. & Hauser, M. D. The auditory behaviour of primates: a neuroethological perspective. *Curr. Opin. Neurobiol.* **11,** 712–720 (2001).
4. Heffner, H. E. & Heffner, R. S. Temporal lobe lesions and perception of species-specific vocalizations by macaques. *Science* **226,** 75–76 (1984).
5. Petersen, M. R., Beecher, M. D., Zoloth, S. R., Moody, D. B. & Stebbins, W. C. Neural lateralization of species-specific vocalizations by Japanese Macaques. *Science* **202,** 324–327 (1978).
6. Hauser, M. D. & Anderson, K. Left hemisphere dominance for processing vocalizations in adult, but not infant, rhesus monkeys: Field experiments. *Proc. Natl Acad. Sci. USA* **91,** 3946–3948 (1994).
7. Phelps, M. E. *et al.* Tomographic measurement of local cerebral glucose metabolic rate in humans with (F-18) 2-fluoro-2-deoxy-D-glucose: Validation of method. *Ann. Neurol.* **6,** 371–388 (1979).
8. Poremba, A. *et al.* Functional mapping of the primate auditory system. *Science* **299,** 568–572 (2003).
9. Ferbert, A. *et al.* Interhemispheric inhibition of the human motor cortex. *J. Physiol. (Lond.)* **453,** 525–546 (1992).
10. Netz, J. in *Transcranial Magnetic Stimulation* (eds Paulus, E., Hallett, M., Rossini, P. M. & Rothwell, J. C.) Ch. 14 (Elsevier Science, New York, 1999).
11. Otten, L. J., Henson, R. N. & Rugg, M. D. Sate-related and item-related neural correlates of successful memory encoding. *Nature Neurosci.* **5,** 1339–1344 (2002).
12. Ehret, G. Left hemisphere advantage in the mouse brain for recognizing ultrasonic communication calls. *Nature* **325,** 249–251 (1987).
13. George, I., Cousillas, H., Richard, J. P. & Hausberger, M. Song perception in the European starling: hemispheric specialization and individual variations. *C. R. Biol.* **325,** 197–204 (2002).
14. Snowdon, C. T., Brown, C. H. & Petersen, M. R. *Primate Communication* (Cambridge Univ. Press, Cambridge, UK, 1982).
15. Hauser, M. D. Functional referents and acoustic similarity: field playback experiments with rhesus monkeys. *Anim. Behav.* **55,** 1647–1658 (1998).
16. Glass, I. & Wollberg, Z. Reponses to cells in the auditory cortex of awake squirrel monkeys to normal and reversed species-specific vocalizations. *Hear. Res.* **9,** 27–33 (1983).
17. Wang, X., Merzenich, M. M., Beitel, R. & Schreiner, C. E. Representation of a species-specific vocalization in the primary auditory cortex of the common marmoset: temporal and spectral characteristics. *J. Neurophysiol.* **74,** 2685–2706 (1995).
18. Rauschecker, J. P. & Tian, B. Mechanisms and streams for processing of "what" and "where" in auditory cortex. *Proc. Natl Acad. Sci. USA* **97,** 11800–11806 (2000).
19. Wang, X. & Kadia, S. C. Differential representation of species-specific primate vocalizations in the auditory cortices of marmoset and cat. *J. Neurosci.* **86,** 2616–2620 (2001).
20. Sokoloff, L., Takahashi, S., Gotoh, J., Driscoll, B. F. & Law, M. J. Contribution of astroglia to functionally activated energy metabolism. *Dev. Neurosci.* **18,** 344–352 (1996).
21. Magistretti, P. Cellular bases of functional brain imaging: insights from neuron-glia metabolic coupling. *Brain Res.* **886,** 108–112 (2000).
22. Woods, R., Mazziotta, J. & Cherry, S. MRI-PET registration with automated algorithm. *J. Comput. Assist. Tomogr.* **17,** 536–546 (1993).
23. Yeterian, E. H. & Pandya, D. N. Corticostriatal connections of the superior temporal region in rhesus monkeys. *J. Comp. Neurol.* **399,** 384–402 (1998).
24. Keppel, G. *Design and Analysis: A Researcher's Handbook*. 2nd edn, Ch. 8 (Prentice-Hall, Englewood Cliffs, NJ, 1982).

Supplementary Information accompanies the paper on **www.nature.com/nature**.

Acknowledgements We thank E. Moreton for programming a software package to phase-scramble the sounds. This work was supported by the Intramural Research Program of NIMH, NIH, DHHS, and by internal funds from the University of Iowa.

Competing interests statement The authors declare that they have no competing financial interests.

Correspondence and requests for materials should be addressed to A.P. (amy-poremba@uiowa.edu).

SOL-1 is a CUB-domain protein required for GLR-1 glutamate receptor function in *C. elegans*

Yi Zheng, Jerry E. Mellem, Penelope J. Brockie, David M. Madsen & Andres V. Maricq

Department of Biology, University of Utah, Salt Lake City, Utah 84112-0840, USA

Ionotropic glutamate receptors (iGluRs) mediate most excitatory synaptic signalling between neurons. Binding of the neurotransmitter glutamate causes a conformational change in these receptors that gates open a transmembrane pore through which ions can pass. The gating of iGluRs is crucially dependent on a conserved amino acid that was first identified in the 'lurcher' ataxic mouse[1]. Through a screen for modifiers of iGluR function in a transgenic strain of *Caenorhabditis elegans* expressing a GLR-1 subunit containing the *lurcher* mutation, we identify suppressor of lurcher (*sol-1*). This gene encodes a transmembrane protein that is predicted to contain four extracellular β-barrel-forming domains known as CUB domains[2,3]. SOL-1 and GLR-1 are colocalized at the cell surface and can be co-immunoprecipitated. By recording from neurons expressing GLR-1, we show that SOL-1 is an accessory protein that is selectively required for glutamate-gated currents. We propose that SOL-1 participates in the gating of non-NMDA (*N*-methyl-D-aspartate) iGluRs, thereby providing a previously unknown mechanism of regulation for this important class of neurotransmitter receptor.

In most nervous systems, fast glutamatergic neurotransmission is mediated by iGluRs that are classified on the basis of their response to the specific ligands NMDA (NMDA receptors), and AMPA (α-amino-3-hydroxy-5-methyl-4-isoxazole propionic acid) and kainate (non-NMDA receptors)[4]. Although many molecules that interact with iGluRs have been described[5], it is likely that additional molecules important for the function of iGluRs remain to be identified. To address this, we undertook a systematic genetic approach to identify genes that are important for non-NMDA iGluR function in the soil nematode *C. elegans*.

Our strategy was based on a gain-of-function mutation found in the lurcher mutant mouse[1]. The mutation is located near the receptor pore region of the GluRδ2 subunit and results in the exchange of a highly conserved alanine for threonine. By an unknown mechanism, this mutation results in both constitutive channel activation and modified gating kinetics[6]. When the homologous mutation is introduced into the *C. elegans* non-NMDA-type GLR-1 subunit[7,8], transgenic nematode worms expressing the modified subunit GLR-1(A/T), referred to here as '*lurcher*' worms, show a marked hyper-reversal behaviour[9]. We used this sensitized genetic background in a screen for suppressors of the *lurcher* movement phenotype. When tested in an assay that measured the time required for a population of worms to reach a